Integrated and multi-scale characterisation of gem materials lacking long-range order. The case studies of chrysocolla and Andean blue opal

New perspectives on structurally complex mineral systems

Sara Monico

Department of Earth Sciences "A. Desio", University of Milano, Via Botticelli 23, 20133 Milano

DOI: 10.19276/plinius.2026.01.012

INTRODUCTION

The gemmological field encompasses a wide variety of materials characterised by remarkable diversity in origin, composition, structure, and physico-chemical properties. Such complexity poses significant challenges for both mineralogical research and gemmological field, particularly with regard to classification, authentication, provenance determination, colour genesis, and the recognition of increasingly sophisticated treatments. Addressing these issues requires advanced analytical methodologies capable of integrating structural, chemical, and textural information across multiple spatial scales (Fritsch et al., 2009; Musa, 2022). This study focuses on a particularly challenging group of gem materials: those lacking long-range structural order. These materials occupy an intermediate stage between crystalline and amorphous systems and are characterised by structural organisation preserved only at short- and medium-range (Rosset et al., 2025). Their complex structural nature, often associated with considerable chemical and textural heterogeneity, limits the effectiveness of conventional analytical approaches and leaves fundamental questions regarding their classification, mineralogical characterisation and formation processes, unresolved. However, these complexities are also the reason behind certain distinctive and highly valued aesthetic qualities of these materials. Specifically, in some cases, these materials are also used in the field of gemmology. Among gem materials lacking long-range structural order, two representative case studies were selected in this study: chrysocolla and a blue variety of opal from Peru. Both are highly valued gemstones, but their mineralogical nature, structural organisation and formation processes have not yet been fully understood, making them ideal case studies for the investigation of materials lacking large-scale structural order.

Chrysocolla, a hydrated copper silicate [$Cu_{2-x}Al_x(H_{2-x}Si_2O_5)(OH)_4 \cdot nH_2O$] (Torpy et al., 2021), is known for its vivid blue-green colour and its millennial use as a pigment and gemstone (Bianucci et al., 2009; Clark, 2021; Torpy et al., 2021). Nevertheless, its classification remains debated in both mineralogy and gemmology because of its variable composition and unresolved structural nature (Frost & Xi, 2013; Torpy et al., 2021; Dold et al., 2023; Kahou et al., 2025). These uncertainties are further compounded by the intrinsic heterogeneity of the material and by the analytical challenges associated with its investigation, including its sensitivity to electron-beam exposure and the limited applicability of conventional crystallographic approaches. To address these unresolved questions, chrysocolla samples from two well-known skarn deposits, Capo Calamita Mine (Elba Island, Italy) and Cornwall Mine (Pennsylvania, USA), were investigated (Fig. 1a).

Opal is a hydrated form of silica ($SiO_2 \cdot nH_2O$) appreciated in jewellery since ancient times for its vivid and various colourations and optical effects (Gliozzo, 2019). It is characterised by variable degrees of structural order, ranging from amorphous varieties, denominated as opal-A, to forms exhibiting a sort of organization, and denominated as opal-CT and opal-C, in which it is possible to recognise the contribution of low-tridymite (T) and/or low-cristobalite-like (C) domains. Despite extensive research, the structural nature of opal remains debated, particularly with regard to -CT and -C types, described by authors throughout a microcrystalline or paracrystalline models (basing on diffraction and spectroscopic data respectively) (Smith, 1998; Curtis et al., 2019; Lee et al., 2022, 2025). Among the many gemmological varieties of opal, Andean blue opal is a distinc-

Figure 1 *Some representative samples investigated in this research project;* ***a)*** *rough samples of chrysocolla from Elba Island and from Pennsylvania;* ***b)*** *rough and polished samples of Andean blue opal.*

tive blue-green variety extracted in southern Peru and of strong cultural value since pre-Hispanic times (Hyršl, 2001; Caucia et al., 2015) (Fig. 1b). It is appreciated for its intense colours, ranging from milky blue to green, yet the causes of its colouration, as well as its structural and compositional characteristics, remain incompletely understood (Gaillou et al., 2008; Caucia et al., 2015). This material occurs in hydrothermal mineralisation associated with the Coastal Batholith of southern Peru, where fluid circulation processes promoted the formation of gem-quality blue opal.

The study of these two varieties therefore addresses unresolved questions in both mineralogy and gemmology. To achieve these objectives, an integrated analytical strategy was developed, combining petrographic observations, advanced structural characterisation, quantitative chemical analyses, multivariate statistical approaches, nanoscale investigations, and thermodynamic modelling. The integration of these complementary datasets provides new constraints on the classification, structural organisation, and formation processes of chrysocolla and Andean blue opal, while contributing to the development of analytical approaches suitable for the investigation of mineral systems lacking long-range structural order.

METHODS

This study adopted an integrated multi-scale analytical workflow specifically designed to investigate gem materials lacking long-range structural order. Given the intrinsic complexity of chrysocolla and Andean blue opal, complementary methods were combined within a hierarchical framework extending from micro- to nanoscale investigations, allowing the correlation of textural, chemical, structural, and genetic information across multiple spatial scales. The investigation started at the Department of Earth Sciences of the University of Milano with optical microscopy observations of polished thin sections, providing the petrographic framework for the study through the identification of textures, mineral associations, internal heterogeneities, and inclusion distributions. Mineralogical characterization was subsequently achieved through the combined use of high-resolution X-ray diffraction (XRD) and micro-Raman spectroscopy. The diffraction data were acquired at the ID22 High Resolution Powder Diffraction beamline (ESRF, France) and at XRD1 beamline at Elettra Sincrotrone Trieste (Trieste, Italy). For chrysocolla, conventional diffraction was complemented by X-ray Total Scattering and Pair Distribution Function (PDF) analyses, enabling the investigation of short- and medium-range structural organization beyond the limits of traditional crystallographic approaches. Micro-Raman spectroscopy and mapping was realized at the Institute of Theoretical and Applied Mechanics of the Czech Academy of Sciences, (Telč Centre, Czech Republic) on thin sections of chrysocolla and opal samples. Chemical characterization was performed using Electron Microprobe Analysis in wavelength-dispersive mode (EMPA-WDS) at the Department of Earth Sciences of the University of Milano, providing quantitative information on major and minor elements. In the case of chrysocolla, particular attention was placed to the optimisation of analytical conditions, and a dedicated analytical setup was developed to minimise beam-induced alteration and ensure reliable quantitative measurements of this highly sensitive material. In the case of Andean blue opal, trace-element concentrations were further investigated by Laser Ablation–Inductively Coupled Plasma–Mass Spectrometry (LA-ICP-MS) at the Laboratory of Geochemistry, Geochronology and Isotopic Geology (LASA labs) of the University of Milano. The resulting datasets were subsequently explored through Principal Component Analysis (PCA), allowing the identification of compositional trends, geochemical groupings, and relationships between chemical variability and mineralogical features. Advanced characterization techniques were employed to investigate structural organization beyond the micrometre scale. Transmission Electron Microscopy (TEM), coupled with EDS analysis, was realized at the Microscopy Platform of the University of Milano-Bicocca (PMiB) and applied to chrysocolla in order to directly examine its nanoscale structure, texture and composition. For Andean blue opal, High-Resolution X-ray Micro-Computed Tomography (micro-CT) were used to reconstruct the spatial distribution of inclusions and to evaluate their relationships with the opaline matrix in three-dimensional perspectives. The analysis was realized at the ID-10 BEATS beamline at the SESAME Synchrotron Radiation Facility (Synchrotron-light for Experimental Science and Applications in the Middle East - Allan, Al Salt, Jordan). Finally, thermodynamic modelling of the Cu-SiO_2-SCOH system (T = 298 K, P = 1 atm) was performed employing *Perple_X* software (Connolly, 2005) to constrain the stability fields of chrysocolla and evaluate the physicochemical conditions associated with its formation.

RESULTS

The integrated analytical approach enabled a comprehensive characterization of chrysocolla and Andean blue opal across multiple scales of investigation.

Chrysocolla

Optical microscopy revealed significant textural variability between the chrysocolla samples from Elba Island and Pennsylvania. In thin section, chrysocolla from Elba Island occurs as arborescent and banded aggregates, commonly associated with opaque Mn-rich phases and secondary Cu minerals. Conversely, the Pennsylvania samples are characterised by predominantly massive and banded textures, locally intergrown with microcrystalline silica bodies and veins. These observations highlight the heterogeneous texture of chrysocolla and the different mineral associations occurring in the two localities.

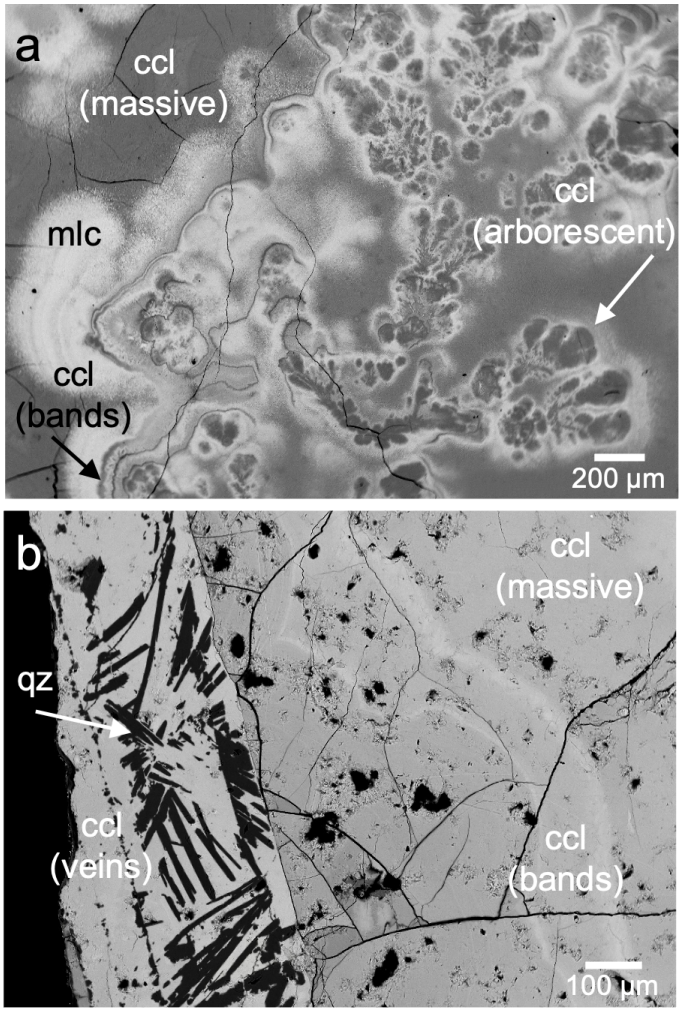

Figure 2 *BSE-SEM images of chrysocolla samples;* ***a)*** *samples from Elba Island and* ***b)*** *from Pennsylvania.*

Micro-Raman spectroscopy revealed highly comparable vibrational signatures for chrysocolla from both localities, indicating a similar local structural organisation despite the marked textural differences observed petrographically. The spectra are characterised by the main chrysocolla bands at ~ 673 cm^{-1} and ~ 643 cm^{-1}, attributed to SiO_3 bending modes, together with signals at ~ 410 cm^{-1} and ~ 1042 cm^{-1} related to SiO_3 bending and stretching vibrations. Raman mapping highlighted distinct mineral associations in the two deposits: chrysocolla is closely associated with malachite and Mn-rich phases in the Elba Island samples, whereas quartz and moganite, occurring as chalcedony, were identified in the Pennsylvania material.

The observation of chrysocolla samples in the BSE-SEM images confimed the observations realized employing the petrographyc microscope, highlighting different microstructures and textures (Fig. 2). Samples from Elba Island show massive, arborescent and banded areas (interspersed with malachite). Samples from Pennsylvania present massive and banded areas, crosscutted by veins of compact chrysocolla (and tabular bodies of microcrystalline and cryptocrystalline silica). EMPA-WDS analyses have revealed that chrysocolla from different locations has a broadly uniform composition, with average CuO and SiO_2 contents of ~ 45.8 wt.% and ~42.0 wt.% in the Elba Island samples, and ~ 41.5 wt.% and ~ 42.8 wt.% in the Pennsylvania ones, respectively. Chrysocolla from Pennsylvania is additionally characterised by higher Al_2O_3 contents (up to ~ 1.3 wt.%) compared to the samples from Elba Island. Principal Component Analysis clearly separated the two groups, defining distinct compositional features and highlinting minor variations among the different chrysocolla textures observed clearly in the BSE images.

High-resolution X-ray diffraction patterns are characterised by broad diffuse features and the absence of sharp Bragg reflections, indicating the lack of well-developed long-range crystalline order. High-resolution total scattering data analysis employing the pair distribution function (PDF) approach has revealed, for the first time, the main Si–O and Cu–O interatomic distances in chrysocolla, which resulted to be ~ 1.59 Å and ~ 1.97 Å, respectively, suggesting a coordination of four. In addition, the PDF signal remains coherent up to approximately 10 Å, demonstrating the persistence of local structural organisation despite the absence of long-range periodicity.

TEM provided direct insights into the nanoscale organisation of chrysocolla (Fig. 3). In samples from both localities, chrysocolla consists predominantly of an intricate network of intergrown nanotubular domains associated with diffuse electron diffraction patterns indicative of limited structural order. The nanotubes occur in denser and less dense regions within the matrix, although no significant chemical differences were detected between them. Locally, the nanotubes are arranged in radial spray, especially in correspondence of banded and arborescent areas observed at the microscale.

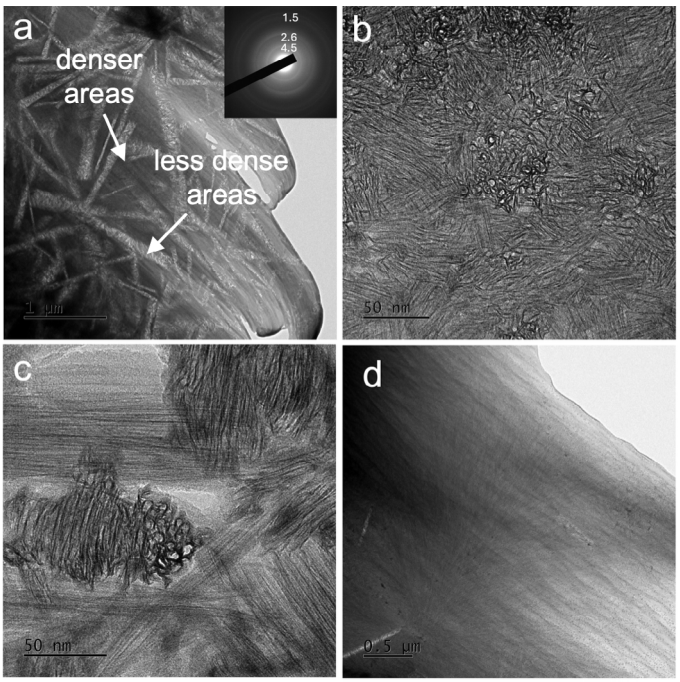

Figure 3 *Bright field (BF)-TEM images of chrysocolla;* ***a)*** *denser and less dense areas of nanotubes;* ***b)*** *nanotubes randomly oriented in chrysocolla samples;* ***c)*** *nanotubes viewed at higher magnification;* ***d)*** *nanotubes arranged in radial spray.*

Andean blue opal

Optical microscopy revealed marked textural variability among the investigated Andean blue opals, allowing the recognition of two main sample groups, named as "Type I" and "Type II". Type I opals are characterised by an undulatory microcrystalline opaline matrix displaying brecciated textures, cryptocrystalline silica veins, alteration relics, and mineral inclusions. In contrast, Type II opals consist of compact silica masses with cryptocrystalline-to-fibrous textures and no observable accessory phases or inclusions.

Consistent with the distinction established by optical microscopy, X-ray diffraction highlighted structural and mineralogical differences between Type I and Type II groups. All samples display in their diffraction patterns the typical broad feature of Opal-CT, located between ~ 4.30 and 4.00 Å (Ghisoli et al., 2010; Curtis et al., 2019). This feature is produced by overlapping tridymite and cristobalite contributions. Nevertheless, differences can be observed in the set of sample patterns. Type I samples are characterised by a main peak centred at approximately 4.09 Å and a relatively intense reflection at approximately 4.28 Å, both indicative of a significant contribution of tridymite (along with broader reflections reflecting a lower structural order). In contrast, Type II samples show a main peak shifted towards approximately 4.05 Å, indicative of a stronger contribution of cristobalite (as well as a higher degree of structural order).

Raman spectroscopy complemented the XRD data by providing insight into the local structural features of opal. The most diagnostic region (200–600 cm^{-1}) (Fig. 4), associated with Si–O–Si and O–Si–O vibrations (Caucia et al., 2021), revealed clear differences between the two groups. Type I samples display a broad band centred at ~ 356 cm^{-1}, together with a secondary signal at ~ 209 cm^{-1}, indicating a predominance of tridymite-like structural domains, consistent with XRD results. In contrast, Type II samples show distinct peaks at ~ 421 and ~ 232 cm^{-1}, accompanied by a signal at ~ 111 cm^{-1}, characteristic of cristobalite-like domains (Ilieva et al., 2007; Balci et al., 2025). The absence of tridymite-related features supports the classification of type II as opal-C. Raman analyses also identified several accessory phases in Type I samples, including chalcedony (quartz + moganite) filling veins and cavities, Fe-bearing phases (hematite and goethite), Mn oxides, and chrysocolla, the Cu-hydrated silicate, recognised by its characteristic band at ~ 673 cm^{-1}. Raman mapping revealed a markedly heterogeneous distribution of chrysocolla, with domains ranging from nearly absent to strongly enriched.

The distinction between the two opal types is also reflected in their chemistry. EMPA-WDS analyses show lower SiO_2 (~ 89 wt.%) and higher MgO and CuO contents in Type I samples, whereas Type II samples are nearly pure silica (~ 98 wt.% SiO_2). BSE imaging revealed widespread chrysocolla and chalcedony veins in Type I samples. PCA of LA-ICP-MS data further separates the two groups, with Type I enriched in Mg, Cu, Zn, V, and U, and Type II associated with Al and Ca. Type I samples also display significant Cu (~ 5400–17,000 ppm) and Fe (~ 9–200 ppm) internal variability.

High-resolution synchrotron tomography was performed on Type I samples to investigate the three-dimensional distribution of mineral phases previously revealed (Fig. 5). In the rough sample (Fig. 5a), chrysocolla forms elongated, preferentially oriented veins that extend throughout the sample (Fig. 5b), consistent with BSE-SEM and petrographic observations. Chalcedony veins crosscut the chrysocolla network, indicating a distinct secondary formation stage (Fig. 5c), whereas Fe-bearing phases are irregularly distributed and show no clear spatial relationship with the other phases (Fig. 5d). Residual porosity is diffuse and mostly disconnected (Fig. 5e), with pore sizes ranging from micrometre to submicrometre scale, suggesting a compact and poorly permeable material.

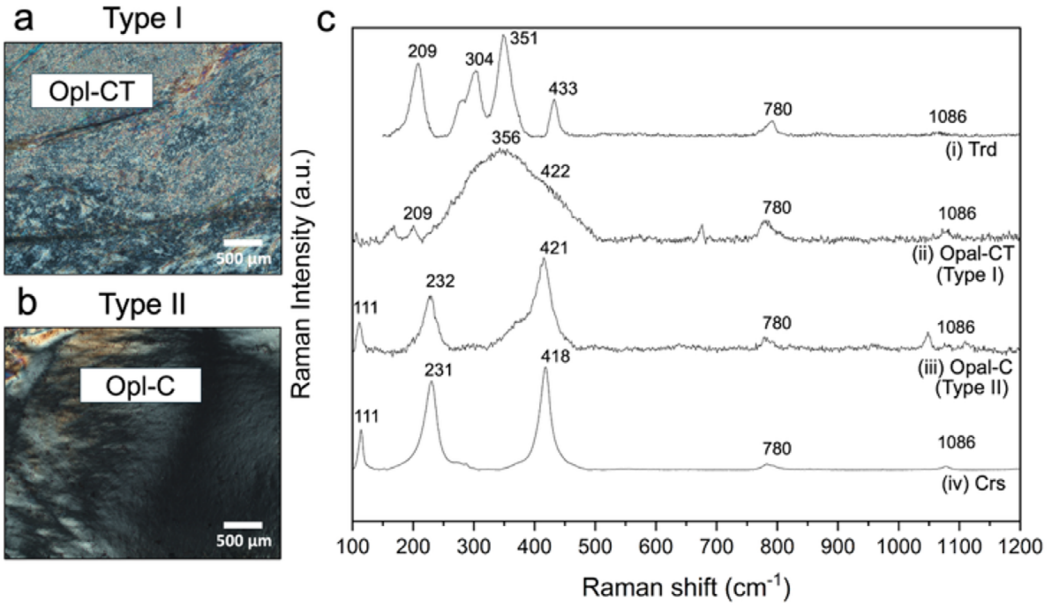

Figure 4 *Micro-Raman Spectroscopy of samples of Andean blue opa.* ***a)*** *Thin sections (XPL) of the first type of samples (Type I) and* ***b)*** *of the second type of samples (Type II) of Andean blue opal.* ***c)*** *Raman spectra in the range 100-1200 cm^{-1} of opal-CT and opal-C compared to the spectra of low-tridymite and low-cristobalite (RRUFF references: R090042 and R060648).*

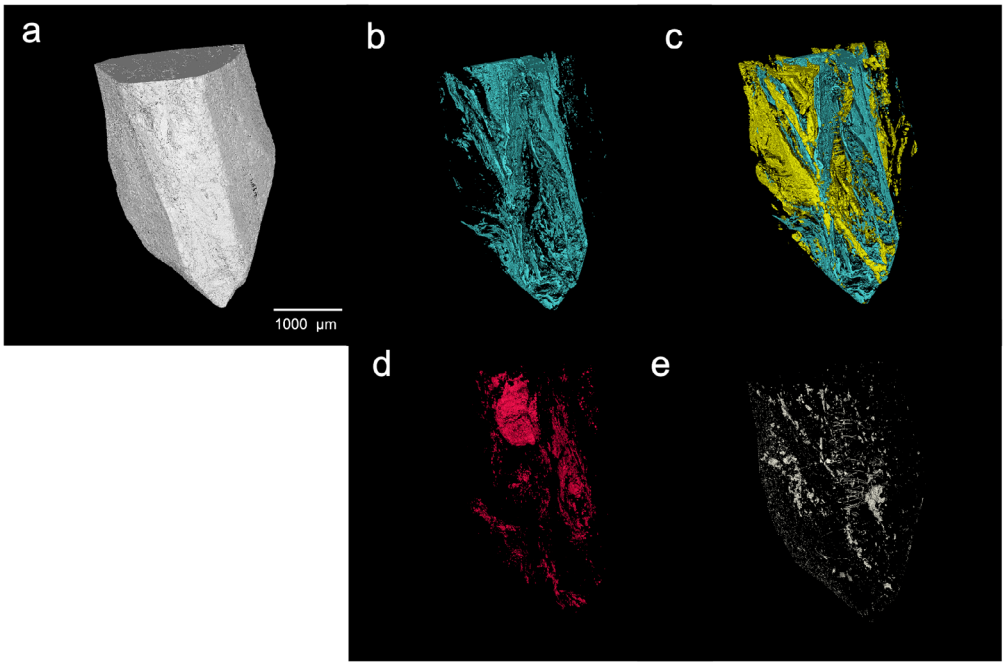

Figure 5 a) *volume rendering of a sample of Type I with the segmentations of mineral phases;* ***b)*** *chrysocolla in veins;* ***c)*** *veins of chalcedony interrupting chrysocolla;* ***d)*** *Fe-rich inclusions irregularly distributed;* ***e)*** *residual porosity.*

DISCUSSION

To summarize, this study provides new insights into chrysocolla. Results highlighted that it is characterised by a relatively homogeneous SiO_2–CuO composition and by structural coherence limited to the short–medium range (~ 10 Å), as revealed by synchrotron total scattering data. While chrysocolla displays highly variable and complex textures at the microscale, TEM observations reveal an intricate network of randomly oriented nanotubes with variable density. Chemical variability is limited and mainly reflects differences in formation environment and mineral associations. To further constrain chrysocolla formation and stability, thermodynamic modelling of the Cu–SiO_2–SCOH system under near-surface conditions ($T \approx 298$ K, $P = 1$ bar) was performed. The resulting predominance diagram (Fig. 6) indicates that chrysocolla is stable under oxidising conditions, requiring Cu^{2+}-bearing fluids and high silica activity similar to that of fluids in equilibrium with quartz or opal (respectively the solid blue line and the dashed blue line in Fig. 6a). This means it forms when silica activity is equal to or higher than quartz saturation. Notably, quartz saturation lies close to the chrysocolla–malachite boundary, implying that small changes in fluid composition can control phase precipitation. This is consistent with the observed chrysocolla–malachite association in Elba samples (Fig. 6b), whereas samples from Pennsylvania shown higher silica activity given the coexistence of chrysocolla and microcrystalline silica phases (Fig. 6c).

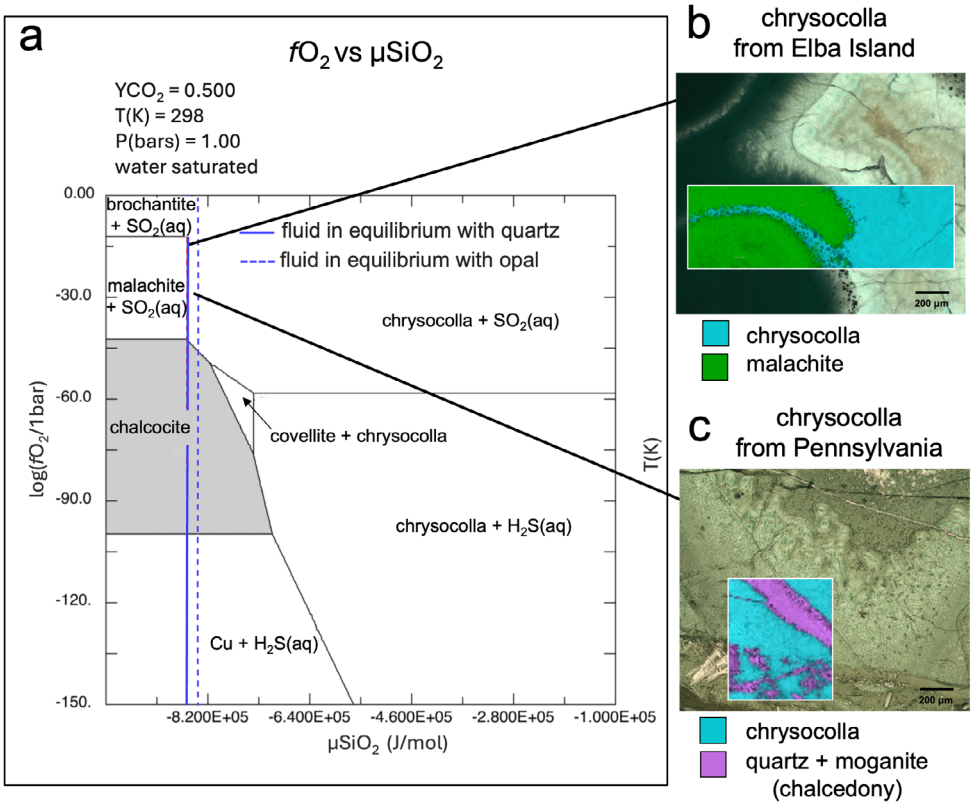

Figure 6 a) *predominance diagram showing the stability fields of copper-bearing minerals as a function of oxygen fugacity (fO_2) and the chemical potential of silica (μSiO_2), at 298 K and 1 bar, with $YCO_2 = 0.5$;* ***b)*** *Raman maps of chrysocolla acquired on the thin section of the sample from Elba Island (chrysocolla associated with malachite) and* ***c)*** *from Pennsylvania (chrysocolla associated with chalcedony).*

This study provides a comprehensive characterisation of Andean blue opal, highlighting the wide internal heterogeneity in terms of structure, composition and texture of this gemmological variety. Specifically, the study has made it possible to distinguish two subcategories of Andean blue opal. XRD shows that both groups belong to the opal-CT field but occupy different positions along the tridymite–cristobalite continuum: Type I is dominated by tridymitic domains and lower structural order, whereas Type II shows a stronger cristobalitic contribution and higher crystallinity. Raman spectroscopy refines this distinction at the local scale, confirming Type I as opal-CT and indicating that Type II approaches, or locally corresponds to, opal-C. This apparent discrepancy of results reflects the different structural scales investigated by the two techniques. Specifically, it highlights how methods sensitive to different length scales provide complementary information on the same structural system. XRD primarily constrains medium-range order and the relative contribution of tridymite- and cristobalite-like domains, whereas Raman spectroscopy probes the local arrangement of SiO_4 tetrahedra, providing information on short-range structural configurations. In this context, the long-standing distinction between microcrystalline and paracrystalline models, derived from diffraction and spectroscopic observations, may be reconciled, as also suggested by Lee et al. (2025), since these models describe complementary aspects of the same system at different structural scales. Taken together, the structural and compositional differences observed between the two groups suggest distinct formation environments. The higher mineralogical complexity of Type I samples, combined with their lower structural order and abundance of accessory phases and impurities, is consistent with precipitation from highly silica-supersaturated fluids undergoing significant chemical evolution through fluid–rock interaction and alteration processes. In contrast, the compositional homogeneity, higher structural organisation, and near-pure silica composition of Type II samples point to precipitation from simpler fluids, dominated by silica, closer to equilibrium conditions and characterised by slower precipitation kinetics. With regard to colouration, the results confirm a fundamental role of copper in both groups. In Type I samples, the blue-green colour is directly linked to the presence of chrysocolla, identified by Raman spectroscopy and shown by Raman mapping to be heterogeneously distributed throughout the opaline matrix. In Type II samples, although Cu^{2+} is present, no Cu-bearing mineral phase was detected, leaving the mechanism responsible for colouration unresolved. Copper may occur as a dispersed impurity within the silica structure or in nanoscale domains below the detection limits of the analytical techniques employed.

CONCLUSIONS

Overall, this study demonstrates how the investigation of gemmological materials lacking long-range crystalline order requires a multidisciplinary and multiscale approach. The integration of complementary analytical techniques enabled the characterisation of chrysocolla and Andean blue opal across different structural, compositional, and textural scales, providing new insights into their nature, classification, colouration, and formation processes. Beyond the specific case studies, this work highlights the value of combining conventional and advanced methodologies to address the complexity of poorly ordered mineral systems. Such approaches not only contribute to resolving open mineralogical questions but also provide a stronger scientific basis for gemmological characterisation and classification.

REFERENCES

Balci, S., Correcher, V., Topaksu, M., Garcia-Guinea, J., Sayin, U. (2025) - Multispectral analysis of natural tridymite: Morphology, composition, and luminescence features. Luminescence, 40, 1-9.

Bianucci, R., Mattutino, G., Lallo, R., Torre, C. (2009) - Identification of a chrysocolla amulet in an Early Dynastic child mummy. J. Archaeol. Sci., 36, 592-595.

Caucia, F., Marinoni, L., Leone, A., Ghisoli, C. (2015) - New physical, geochemical and gemological data of opals from Acari Mine (Arequipa Department, Peru). NEUES JB MINER ABH, 192, 73-84.

Caucia, F., Marinoni, L., Gilio, M., Dal Corso, E. (2021) - Characterization of recently discovered common green opals from Anosy (Madagascar). Period. Mineral., 90, 217-228.

Clark, M. (2021) - Gemstones and the artist's palette – Natural mineral colouring of paint pigments. Aust. Gemmol., 27, 330–342.

Connolly, J.A. (2005) - Computation of phase equilibria by linear programming: a tool for geodynamic modeling and its application to subduction zone decarbonation. Earth Planet. Sci. Lett., 236, 524-541.

Curtis, N.J., Gascooke, J.R., Johnston, M.R., Pring, A. (2019) - A review of the classification of opal with reference to recent new localities. Minerals, 9, 299.

Dold, B., Pinget, M.C., Fontboté, L. (2023) - Genesis of the exotic chrysocolla– "copper pitch/wad"–atacamite/brochantite ore at the Exótica (Mina Sur) deposit, Chuquicamata, Chile. Miner Deposita, 58, 569–591.

Fritsch, E., Rondeau, B. (2009) - Gemmology: The developing science of gems. Elements, 5, 147–152.

Frost, R.L., Xi, Y. (2013) - Is chrysocolla $(Cu,Al)_2H_2Si_2O_5(OH)_4{\cdot}nH_2O$ related to spertiniite $Cu(OH)_2$? – A vibrational spectroscopic study. Vib. Spectrosc., 64, 33–38.

Ghisoli, C., Caucia, F., Marinoni, L. (2010) - XRPD patterns of opals: A brief review and new results from recent studies. Powder Diffr., 25, 274–282.

Gliozzo, E. (2019) - Variations on the silica theme: Classification and provenance from Pliny to current supplies. In "Silica: Physical behavior, geochemistry and materials applications" P. Ballirano, M. Capitani, & D. Bersani eds. EMU notes in mineralogy, 20, 13–85.

Gaillou, E., Delaunay, A., Rondeau, B., Bouhnik-le-Coz, M., Fritsch, E., Cornen, G., Monnier, C. (2008) - The geochemistry of gem opals as evidence of their origin. Ore Geol. Rev., 34, 113–126.

Hyršl, J. (2001) - Gemstones of Peru. J. Gemmol., 27, 328–334.

Ilieva, A., Mihailova, B., Tsintsov Z., Petrov, O. (2007) - Structural state of microcrystalline opals: A Raman spectroscopic study. Am. Mineral, 92, 1325–1333.

Kahou, Z.S., Seydoux-Guillaume, A.M., Zanetta, P.M., Duchêne, S., Brichau, S., Campos, E. (2025) - Nanoscale characterization of chrysocolla, black chrysocolla and pseudomalachite from 2 supergene copper deposits of Atacama Desert of northern Chile. Am. Mineral., 110, 1329–1339.

Lee, S., Xu, H., Xu, H. (2022) - Reexamination of the structure of opal-A: A combined study of synchrotron X-ray diffraction and pair distribution function analysis. Am. Mineral., 107, 1353–1360.

Lee, S., Xu, H., Xu, H., Xu, W. (2025) - Reexamination of the structure of nanomineral opal-CT using synchrotron X-ray diffraction, transmission electron microscopy, X-ray scattering structure factor, and pair distribution function analyses. Am. Mineral., 110, 721–730.

Musa, M. (2022) - The importance of multidisciplinary analytical strategies to solve identification and characterization challenges in gemology: The example of the "green stones". Appl. Sci., 12, 11767.

Rosset, L.A., Drabold, D.A., Deringer, V.L. (2025) - Signatures of paracrystallinity in amorphous silicon from machine-learning-driven molecular dynamics. Nat. Commun., 16, 2360.

Smith, D.K. (1998) - Opal, cristobalite, and tridymite: Noncrystallinity versus crystallinity, nomenclature of the silica minerals, and bibliography. Powder Diffr., 13, 2–19.

Torpy, A., Fan, R., Wilson, N., MacRae, C., Austin, P. (2021) - Quantifying trace element variations in chrysocolla by clustering FEG-EPMA hyperspectral maps. Microsc. Microanal., 27, 1870–1872.

Umpleby, J.B. (1914) - Crystallized chrysocolla from Mackay, Idaho. Proc. Wash. Acad. Sci., 4, 181–183.